19th WORLD CONFERENCE OF THE ASSOCIATED RESEARCH CENTRES FOR THE URBAN UNDERGROUND SPACE
Belgrade, Serbia, November 4-7, 2025.

ACUUS BELGRADE 2025

Paper No: 2.10.150
DOI: 10.46793/ACUUS2025.2.10.150

IDENTIFICATION OF KARST CAVES BASED ON MULTI-SOURCES DATA FUSION DURING SHIELD TUNNELLING

Xin-Hao Min[1], Yan-Ning Wang[2], Shui-Long Shen[3]

Abstract: This study proposes an enhanced method that integrates KCII with the Energy per Revolution Index (EPRI) derived from shield operational parameters. The method fuses operational parameters such as thrust, torque, cutterhead rotational speed, advance rate, soil chamber pressure, and penetration rate. Data are processed based on each cutterhead revolution, which represents dynamic characterization of geological conditions ahead of the tunnel face. A sliding window approach calculates the mean and standard deviation of KCII and EPRI to establish identification thresholds. Four distinct identification logics are developed and evaluated: KCII only, dual conditions of EPRI indicators, a combined approach of all indicators, and any two indicators. Application to two sections of Xuzhou Metro Line 4 validates method effectiveness and demonstrates high accuracy and robust generalization. Results shows that the multi-indicator fusion logic significantly improves accuracy compared to single-indicator methods, and offers real-time geological insights to support safer and more efficient shield tunnelling operations.

Keywords: Shield tunnelling, Karst strata, Earth pressure balance, Shield parameters, Identification method

1. INTRODUCTION

Shield tunnelling technology has become indispensable in modern urban infrastructure development, particularly when navigating complex geological conditions like karst regions (Peng et al., 2023). Karst caves present significant risks, such as water inrush, collapse, and equipment damage, requiring precise real-time identification and management (Cho et al., 2021). However, conventional geological exploration methods, including borehole drilling and advanced geological forecasting, face critical challenges such as limited resolution, high operational cost, and delayed identification capability (Li, et al., 2017; Ghosh et al., 2018; Chen et al., 2021).

To tackle the energy consumption during shield tunnelling, Teale (1965) proposed an index called Specific Energy (SE) based on energy analysis. Tarkoy and Marconi (1991) proposed another index, FPI, based on stress state analysis. Yamamoto et al. (2003) proposed TPI to evaluate the geological condition ahead of the tunnel face. Yan et al. (2023) proposed a more generalized index, GFII, to identify the geological characteristics when a shield is passing through a mixed soi-rock strata. Among these, the Karst Cave Identification Index (KCII) offered improved geological recognition capabilities. Despite this advancement, KCII remained primarily qualitative, limiting its effectiveness in dynamic operational environments due to insufficient temporal resolution and quantitative characterization capabilities.

To overcome these limitations, this study proposes a novel approach integrating KCII with a newly developed Energy per Revolution Index (EPRI), calculated using real-time shield tunnelling parameters. This integrated method provides high-frequency, quantitative monitoring of geological changes based on the energy consumed per cutterhead revolution, enhancing the detection sensitivity and accuracy of karst cave identification. Furthermore, a sliding window algorithm and multiple logic scenarios are applied to establish robust criteria for distinguishing karst features from intact rock formations.

[1] Ph.D. Candidate, Min, Xin-Hao, B.Eng. Civil Engineering, Shantou University, Shantou, China; 21xhmin@stu.edu.cn.
[2] Assc. Prof., Wang, Yan-Ning, Ph.D. Civil Engineering, College of Engineering, Shantou University, Shantou, China, wangyn@stu.edu.cn.
[3] Professor, Shen, Shui-Long, Ph.D. Civil Engineering, Dean College of Engineering, Shantou University, Shantou, China, shensl@stu.edu.cn.

The effectiveness of the proposed methodology is demonstrated through extensive field application in the Xuzhou Metro Line 4. Comparative analysis confirms that the multi-indicator approach not only significantly improves detection accuracy but also enhances the method's adaptability and generalization across different geological conditions. This comprehensive, quantitative approach contributes to safer tunnelling practices and provides valuable insights for geological risk management during construction.

2. MATERIAL AND METHODS

2.1. Data Acquisition and Pre-processing

In this study, the shield machine parameters, including the thrust (F), torque (T), cutterhead rotational speed (CRS), advance rate (AR), soil-chamber pressure (P) and penetration rate (PR), were automatically recorded and saved during construction. For each second, the instantaneous angular increment of the cutterhead is $\Delta\theta = CRS/60 \times 360°$. The cumulative angle $\Sigma\theta$ is reset whenever it exceeds 360°, and the elapsed seconds define the duration of one complete revolution. All raw measurements within that interval are averaged, yielding a revolution-based dataset that synchronises mechanical response with the excavation face.

2.2. Identification indices

Wang et al. (2025) established the mechanical equilibrium conditions required for tunnel face stability based on the earth pressure balance principle and proposed the Karst Cave Identification Index (KCII) as a novel evaluation indicator. The dimensionless KCII is computed as:

$$KCII = \frac{P \cdot CRS \cdot V_e}{F \cdot AR} \tag{1}$$

where F is the thrust of the shield machine (kN), AR is the advance rate (m/s), CRS is the cutterhead rotational speed (r/s), P is the soil pressure in soil chamber (kPa), and V_e is the volume of the soil chamber (m^3).

Specific Energy (SE) quantifies the energy required to excavate a unit volume of soil/rock. The formula of SE is as follows:

$$SE = \frac{F}{A} + \frac{2\pi \cdot CRS \cdot T}{A \cdot AR} \tag{2}$$

where SE is the Specific Energy (SE) of the shield machine, F is the thrust (N); A is the cutterhead area (m2); CRS is the cutterhead rotational speed (r/s); T is the cutterhead torque (N.m); AR is the advance rate (m/s).

However, its conventional formulation necessitates the complete excavation of one cubic meter of material to compare energy dissipation across the tunnel face, rendering it incapable of real-time geological assessment via energy fluctuations. Based on the time it takes for the cutterhead to rotate once, the energy consumption per unit volume is converted into an Energy per Revolution Index (EPRI) that is related to time. The formula is as follows:

$$EPRI = F \times AR \times 16.7 + T \times CRS \times 1.05 \tag{3}$$

the rate of change of energy consumption per revolution of the cutter head, ΔEPRI is:

$$\Delta EPRI = \frac{\Delta E_{total}}{\Delta t} = \frac{EPRI_2 - EPRI_1}{\Delta t \cdot EPRI_1} \tag{4}$$

2.3. Identification method

A sliding window of three consecutive revolutions traverses the index time series. Within each window, the mean and standard deviation of KCII, EPRI and ΔEPRI are computed in real time. Thresholds for the three indices are derived from a benchmark window located entirely within a karst cavity confirmed by borehole evidence, and these thresholds are then used as fixed references for subsequent detection. Each window is classified under four

decision schemes: KCII only; EPRI together with ΔEPRI; all three indices jointly; any two indices. Windows that satisfy the selected scheme are labelled as cave; all other windows are labelled as intact rock.

2.4. Project background

Figure 1 shows the locations and geological conditions of the two research sections of the Xuzhou Metro Line 4 where this method was applied. Sections 337-345 constitute Area A, while sections 460-470 constitute Area B. Each of these areas contains a detected cave. The cave in Area A measures: width x height = 4.2 x 6.2 (m), approximately in the range of 340-344; the cave in Area B measures: width * height = 3.6 x 4.5 (m), approximately in the range of 463-468. Both caves are within the tunnel's influence area.

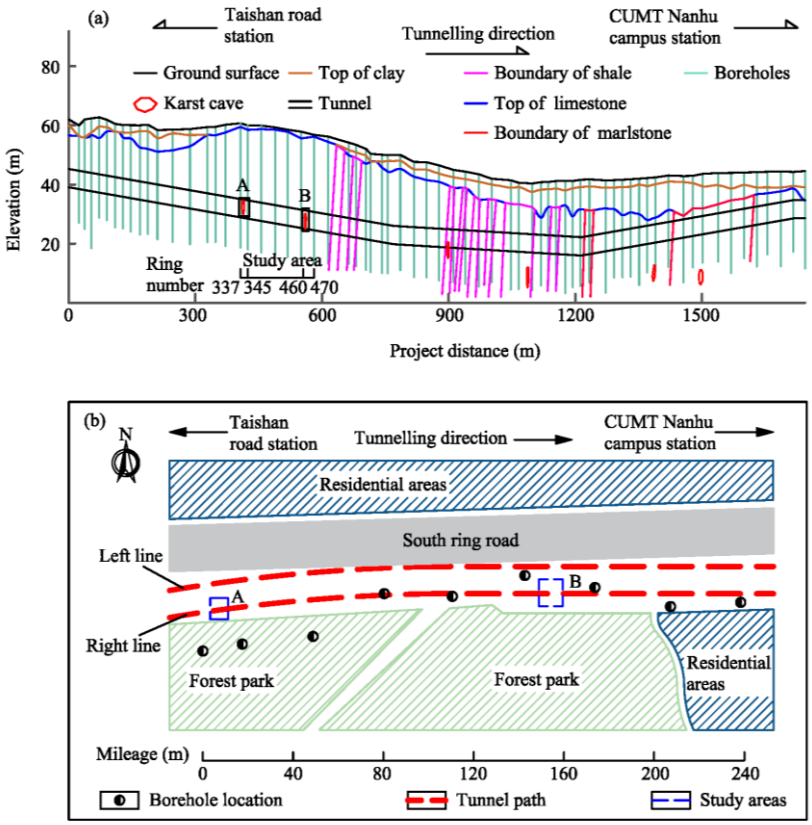

Figure 1. *Overview of study area: (a) plane position diagram and (b) geological profiles with the area ratio of the cave in the tunnel*

3. RESULTS

3.1. Indices calculation

Figure 2 shows the calculation results of the three indicators, as well as the relationship between these results and time and geological features. In the karst-affected zones of Study Area A, analysis reveals a mean KCII value of 0.04. The EPRI demonstrates substantial volatility with a mean of 2,349,650 kJ/rev and a standard deviation of 488,620. Conversely, the ΔEPRI metric exhibits minimal variation, registering a mean of 0.00014 with a standard deviation of 451,909.

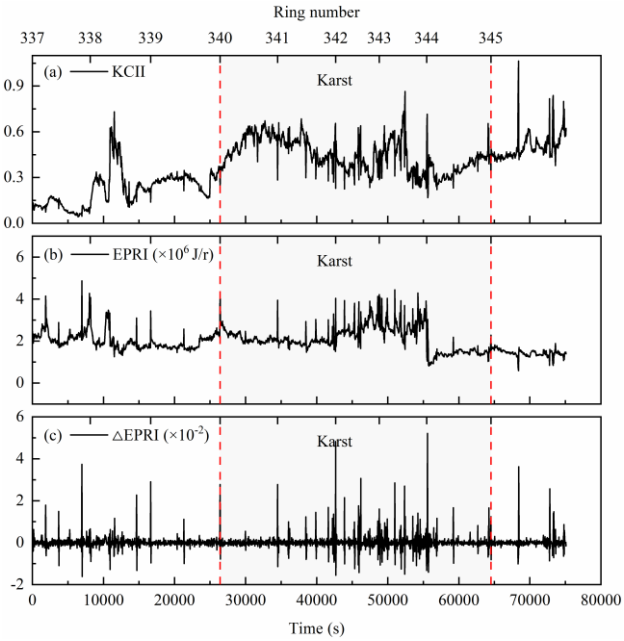

Figure 2. *Calculation results of indicators in study area A*

3.2. Accuracy rate of stratum identification

Figures 3 and **4** summarise the recognition performance of four logical schemes in the calibration zone, rings 337 to 345, and the validation zone, rings 460 to 470, respectively. In **Figure 3**, the highest overall accuracy, 76.3 %, is attained by Logic D, the any two indices scheme, which balances sensitivity in the cavity with specificity outside it, whereas Logic A, the KCII only scheme, captures the cavity most effectively with a hit rate of 70.0 %. **Figure 4** shows that applying the same thresholds to an independent geological segment leads to a decline in overall accuracy; nevertheless, Logic A achieves the best whole section score, 63.0 %, and maintains accuracy outside the cavity above 96 %. These trends indicate that indicator redundancy improves robustness in the learning zone, while KCII alone remains the most portable cue for unseen ground conditions.

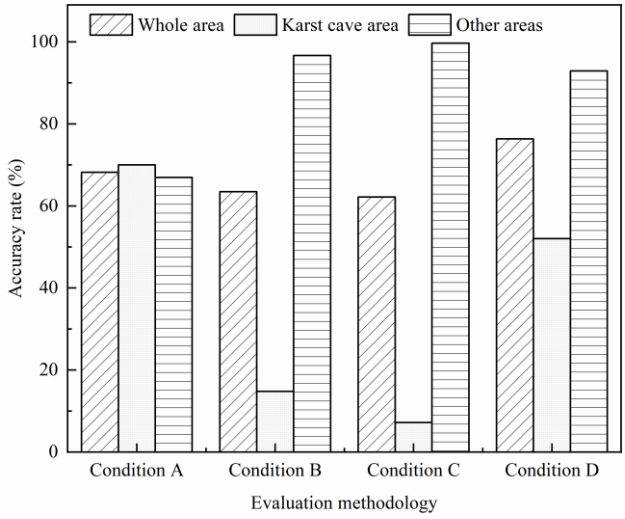

Figure 3. *Accuracy rate of identification in Area A*

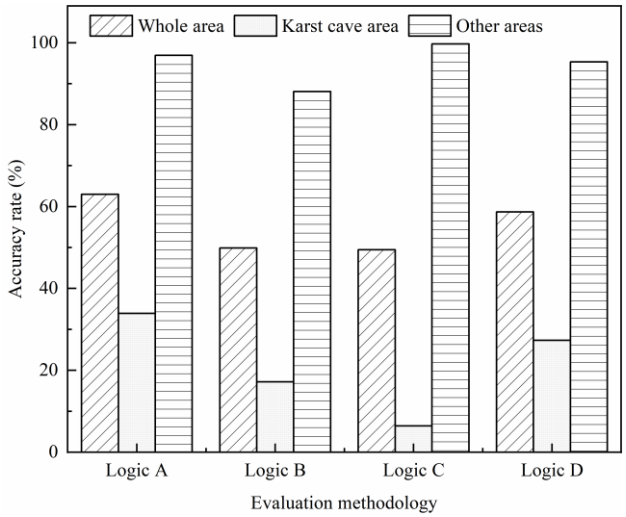

Figure 4. *Accuracy rate of identification in Area B*

4. DISCUSSION

The field application confirms that per-revolution resampling effectively captures the response of the cutterhead. This resampling also removes high-frequency noise that masks geological signals. Within this framework, KCII reflects stress equilibrium at the excavation face. EPRI and its normalized increment (ΔEPRI) detect rapid energy changes due to lithological differences. These combined indices provide a comprehensive diagnostic capability superior to any single indicator.

In the calibration zone (rings 337–345), Logic D (any two indices) achieves the highest overall accuracy (approximately 76%). This indicates index redundancy enhances robustness when thresholds are set locally. Logic A (KCII-only) shows the highest detection rate within the cavity. Logic C (all three indices) minimizes false positives in intact rock. Therefore, the choice of logic depends on whether higher sensitivity or specificity is required during construction.

Testing thresholds on an independent section (rings 460–470) highlights threshold portability. Overall accuracy declines to approximately 63% under Logic A. However, the false-positive rate outside cavity zones remains below 4% with Logic C. This result shows sliding-window statistics remain robust across intact rock zones. However, reduced sensitivity within cavities suggests thresholds need adaptive adjustment or integration with machine-learning techniques for geological conditions varying significantly in stiffness or fill properties.

The method shows strong karst-cavity discrimination in this project. Subsequent work will investigate its application to other projects to further improve the method's applicability.

5. CONCLUSION

This study proposes an real-time karst-cave identification in shield tunnelling by integrating per-revolution resampling with a tri-index diagnostic system (KCII, EPRI, ΔEPRI) and a sliding-window decision algorithm. Application to two segments of Xuzhou Metro Line 4 shows the reliability and transferability of the proposed method. Per-revolution resampling aligns shield parameters with excavation-face mechanics, which ensures accurate identification indices computations without extra instrumentation. A 3-revolution sliding window is calibrated using data from a known cavity. This window distinguishes anomalous energy signatures. Logic D achieves the highest overall accuracy (76%). Logic C effectively reduces false positives to below 4% in intact rock. Although thresholds derived from one cavity maintain acceptable performance in other sections, detection sensitivity decreases, suggesting adaptive thresholding refinement as necessary for varied geological conditions. The method's adaptability in international contexts will be further investigated in future work.

6. ACKNOWLEDGEMENTS

The research work was funded by Guangdong Provincial Basic and Applied Basic Research Fund Committee (2022A1515011200), Science and Technology Planning Project of Guangdong Province of China

(STKJ2021129), Research on intelligent construction technology and key control technology of shield tunnel for protecting environment in karst area (CR17GD-GD-XZ6103-JSFW-2023-001).

7. BIBLIOGRAPHY

[1] Chen, Z., Zhang, Y., Li, J., Li, X., Jing, L. (2021). Diagnosing tunnel collapse sections based on TBM tunnelling big data and deep learning: A case study on the Yinsong Project, China. Tunnelling and Underground Space Technology, 108, 103700. https://doi.org/10.1016/j. tust.2020.103700.

[2] Cho, J.W., Jeon, S., Yu, S.H., Chang, S.H. (2010). Optimum spacing of TBM disc cutters: A numerical simulation using the three-dimensional dynamic fracturing method. Tunnelling and Underground Space Technology, 25, 230-244. https://doi.org/10.1016/j.tust.2009.11.007.

[3] Ghosh, R., Gustafson, A., Schunnesson, H. (2018). Development of a geological model for chargeability assessment of borehole using drill monitoring technique. International Journal of Rock Mechanics and Mining Sciences, 109, 9-18. https://doi.org/10.1016/j.ijrmms.2018.06.015

[4] Li, S.C., Liu, B., Xu, X.J., Nie, L.C., Liu, Z.Y., Song, J., Sun, H.F., Chen, L., Fan, K.R. (2017). An overview of ahead geological prospecting in tunnelling. Tunnelling and Underground Space Technology, 63, 69-94. https://doi.org/10.1016/j.tust.2016.12.011

[5] Tarkoy, P.J., Marconi, M. (1991). In: Difficult Rock Comminution and Associated Geological Conditions. Institute of Mining and Metallurgy, London, pp. 195–207.

[6] Teale, R. (1965). The concept of specific energy in rock drilling. International Journal of Rock Mechanics and Mining Sciences & Geomechanics Abstracts 2 (1), 57–73. https://doi.org/10.1016/0148-9062(65)90022-7

[7] Yamamoto, T., Shirasagi, S., Yamamoto, S., Mito, Y., Aoki, K. (2003). Evaluation of the geological condition ahead of the tunnel face by geostatistical techniques using TBM driving data. Tunnelling and Underground Space Technology 18 (2–3), 213–221. https://doi.org/10.1016/S0886-7798(03)00030-0

[8] Yan, T., Shen, S.L., Zhou, A. (2023). GFII: A new index to identify geological features during shield tunnelling. Tunnelling and Underground Space Technology, 142, 105440. https://doi.org/10.1016/j.tust.2023.105440